Screening and Identification of Hypoxia-Inducible Factor Signaling Inhibitor with Antiangiogenic Activity

Chao Li[1#] Yuanzheng Wei[2#] Ping Wang[1#] Xiaoxian Xue[1] Guangyao Wei[3] Mu Chen[4] Xinyun Zhang[5] Lei Cai[2] Yu Zhang[2] Xumu Zhang[1*] Yingjun Li[1,6*]

[1] Department of Chemistry and Medi-X Pingshan, Southern University of Science and Technology, Shenzhen, People's Republic of China
[2] Guangdong Province Key Laboratory of Laboratory Animals, Guangdong Laboratory Animals Monitoring Institute, Guangzhou, Guangdong, People's Republic of China
[3] Advanced Medical Research Institute, Cheeloo College of Medicine, Shandong University, Jinan, People's Republic of China
[4] Guangzhou Municipal and Guangdong Provincial Key Laboratory of Molecular Target & Clinical Pharmacology, the NMPA and State Key Laboratory of Respiratory Disease, School of Pharmaceutical Sciences and the Fifth Affiliated Hospital, Guangzhou Medical University, Guangzhou, People's Republic of China
[5] ICE Bioscience Incorporated Company, Beijing, People's Republic of China
[6] State Key Laboratory of Respiratory Disease, The First Affiliated Hospital of Guangzhou Medical University, Guangzhou Medical University, Guangzhou, People's Republic of China

Address for correspondence Xumu Zhang, PhD, Department of Chemistry, and Medi-X Pingshan, Southern University of Science and Technology, 1088 Xueyuan Avenue, Shenzhen 518000, People's Republic of China (e-mail: zhangxm@sustech.edu.cn).

Yingjun Li, PhD, State Key Laboratory of Respiratory Disease, The First Affiliated Hospital of Guangzhou Medical University, Guangzhou Medical University, 195 Dongfeng Xi Road, Guangzhou 510182, People's Republic of China (e-mail: liyjun@gzhmu.edu.cn).

Pharmaceut Fronts 2024;6:e421–e429.

Abstract

Hypoxia-inducible factors (HIFs) play a key role in regulating cellular responses to low-oxygen conditions, particularly in promoting angiogenesis in tumor microenvironments. Aberrant HIF signaling enhances tumor growth and contributes to resistance against chemotherapy and radiotherapy. Targeting the HIF pathway has emerged as a promising strategy for cancer therapy. This study aimed to identify novel inhibitors of HIF signaling and evaluate their potential against the HIF–vascular endothelial growth factor (VEGF) axis for antiangiogenic therapy. In screening our in-house drug library using hypoxia response element dual-luciferase assay, HST3782, a novel 3-hydroxy-8-azabicyclo[3.2.1]octane-bridged compound, was identified as a promising HIF inhibitor, with IC_{50} of 1.028 μmol/L. In this work, the inhibitory effect of HST3782 on HIF signaling was confirmed in triple-negative breast cancer cells (SUM159) under hypoxic conditions (1% O_2). Quantitative real-time polymerase chain reaction suggested the inhibitory effect of HST3782 on the expression of angiogenic genes, including VEGFa, VEGFR-1, BNIP3, and SERPINE1 in 786-O cells. Zebrafish model testing revealed that HST3782 inhibited intersegmental and subintestinal vessel development by up to 56% without marked toxicity. HST3782 was synthesized through a two-step 1,2,4 triazole cyclization reaction, followed by amide

Keywords
- hypoxia-inducible factor
- HIF pathway inhibitor
- angiogenesis
- zebrafish
- bridged compound

[#] *These authors contributed equally to this work.*

received
April 4, 2024
accepted
November 5, 2024
article published online
December 9, 2024

DOI https://doi.org/10.1055/s-0044-1796627.
ISSN 2628-5088.

Georg Thieme Verlag KG, Rüdigerstraße 14, 70469 Stuttgart, Germany

formation and ketone reduction steps. The last step of hydrogenation with sodium borohydride yielded a pair of endo-exo isomers. 2D-NOESY (Nuclear Overhauser effect spectroscopy) analysis confirmed that the compound's endo isomer (HST3782) had superior inhibitory effects relative to its exo form (**8b**). Given the above, HST3782 is a novel HIF inhibitor, with strong antiangiogenic effects and presents a valuable scaffold for future development of antiangiogenic drugs targeting the HIF–VEGF axis. Further studies are warranted to optimize HST3782's pharmacokinetics and therapeutic efficacy for antiangiogenic therapy in hypoxia-related malignancies.

Introduction

Hypoxia, characterized by decreased intracellular oxygen levels, is associated with the development of malignancy, and resistance to radiation and chemotherapy, and predicts poor outcomes in various tumor types.[1,2] Hypoxia-inducible factors (HIFs), the mast regulator in the response to hypoxia, consist of three inducible α-subunits (HIF-1α, HIF-2α, and HIF-3α) and one constitutively expressed β-subunit (HIF-1β or arylhydrocarbon receptor nuclear translocator).[3–5] Under normal oxygen conditions, HIF-α subunits undergo rapid hydroxylation at specific proline residues by HIF-prolyl hydroxylases, which was subsequently degraded via the von Hippel–Lindau tumor suppressor gene product (pVHL)-mediated ubiquitin–proteasomal pathway.[6,7] Upon hypoxic stabilization, HIF-α accumulates and forms transcriptional complexes with HIF-1β translocates to the nucleus to bind to hypoxia response elements (HREs) and induce the expression of downstream genes involved in cell survival, proliferation, angiogenesis, and metabolic reprogramming.[8,9] The HIF pathway is a positive regulator of the malignant phenotype and regulates multiple aspects of tumorigenesis, making it a critical target for antitumor therapy.

In the tumor hypoxic microenvironment, HIF plays a critical role in enhancing glucose metabolism and vascular endothelial growth factor (VEGF) expression to facilitate angiogenesis, enabling cells to adapt to low oxygen levels. HIF signaling promotes angiogenesis by inducing VEGF transcription, facilitating endothelial cell migration to hypoxic regions.[10] Thus, targeting the HIF–VEGF axis emerged as a promising therapeutic strategy for cancer treatment, with significant efforts focused on developing HIF inhibitors. PT2399, also known as belzutifan and MK-6482, is a small-molecule inhibitor that binds directly to HIF-2α and disrupts its interaction with HIF-1β has been approved for treating patients with VHL disease associated with renal cell carcinoma or pancreatic neuroendocrine tumors since 2022.[11,12] Antitumor drugs topotecan suppressed HIF-1α and resulted in a decrease in VEGF expression in both *in vivo* and *in vitro* assays.[13] The proteasome inhibitor anticancer drug bortezomib (PS-341) was reported to repress HIF-1α protein expression and nuclear accumulation by inhibiting both PI3K/Akt/mTOR and MAPK pathways in prostate cancer.[14–16] Additionally, various compounds, including acriflavine, (*E*)-phenoxyacrylic amide derivatives, chalcone derivatives, and benzofuran derivatives, have been identified as potential HIF inhibitors with antiangiogenic properties, offering potential for the development of novel cancer therapeutics.[17–20] Herein, we screened our compound collections and identified HST3782, a 3-hydroxy-8-azabicyclo[3.2.1]octane bridged compound, as a novel HIF inhibitor with interesting scaffold. HST3782 effectively suppressed HIF-targeted gene expression, including VEGFa and VEGFR, and potently inhibited the angiogenesis and vasculature in zebrafish models, demonstrating its potential for further development.

Results and Discussion

To identify novel scaffolds targeting the HIF pathway, we developed a dual-luciferase screening assay using our compound collection. Initially, primary clear cell adenocarcinoma cell line 786-O cells that harbored mutated VHL-1 and exhibited constituted active HIF-2α signals were transiently transfected with the HER-Luc2 vector and renilla control vector. The collection of about 100 molecules was screened with a concentration of 10 μmol/L and the luciferase signals were measured 48 hours after drug incubation. The HRE luciferase signals were normalized with the control renilla signals. Among the compounds tested, HST3782 emerged as a potent inhibitor at 10 μmol/L. Subsequently, it was tested in a multiple-dosed assay along with PT2385, a validated and commercially available HIF-2α inhibitor.[21] The result showed that HST3782 dose-dependently inhibits HIF signaling with an IC_{50} of 1.028 μmol/L.

Targeting the HIF pathway represents a potential new strategy for refractory triple-negative breast cancer therapy.[22] Next, we assessed the effects of HST3782 on the HIF pathway in the triple-negative breast cancer cell line SUM159 (►**Fig. 1A**). These cells were transfected with HRE-Luc2 and renilla vectors under both normoxic (21% O_2) and hypoxic (1% O_2) conditions.[22] Consistent with previous reports, hypoxia-activated the HIF pathway, resulting in a significant increase in HRE reporter signals. Treatment with 10 and 20 μmol/L HST3782 led to a reduction in HIF signaling by 74 and 80%, respectively; whereas the HIF signal inhibitor acriflavine at 5 μmol/L suppressed HIF signaling by 90%.

After demonstrating the inhibitory effect of HST3782 against the HIF reporter, a quantitative real-time PCR was conducted to assess the expression of HIF downstream genes in 786-O cells with additional HST3782 treatment. The result showed that 10 μmol/L HST3782 effectively inhibited the expression of VEGFa,

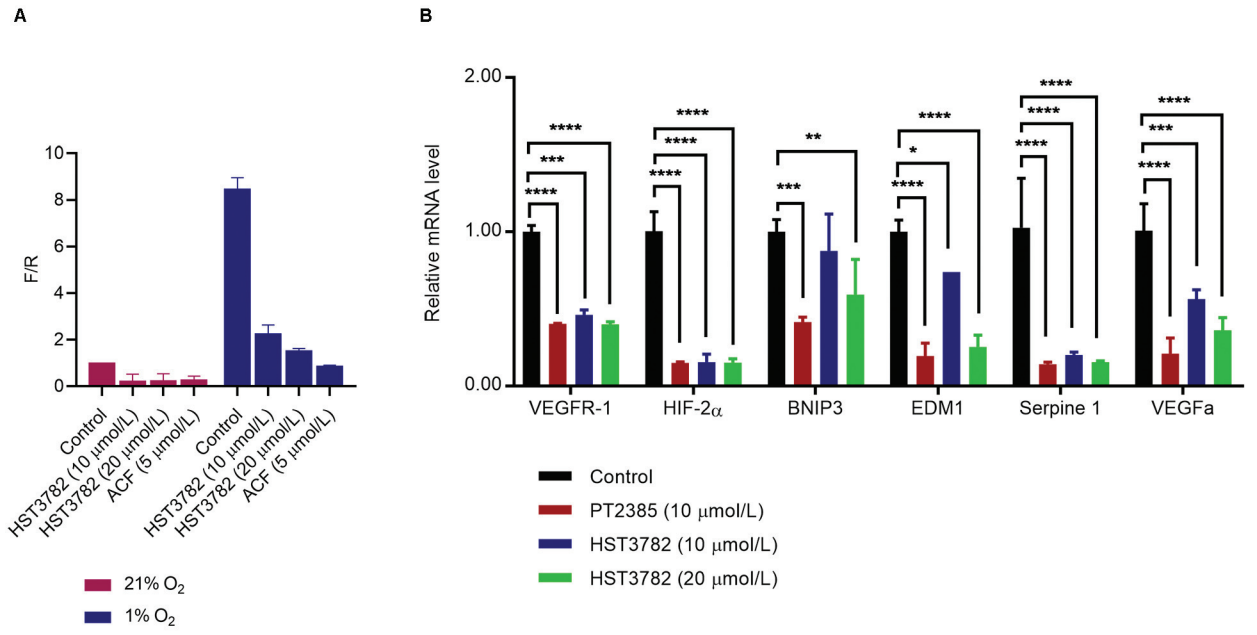

Fig. 1 Screening and the characterization of HST3782 as a HIF signaling inhibitor. (**A**) The inhibition of HRE dual-luciferase reporters of HST3782 in SUM159 cells. (**B**) The downregulation of HIF-2α regulated gene in 786-O cells. Data are expressed as the mean ± standard deviation ($n = 10$). $^{*}p < 0.05$, $^{**}p < 0.01$, $^{***}p < 0.001$, $^{****}p < 0.0001$ versus the control group (cells treated with the same volume of DMSO instead of a drug), analyzed by two-tailed Student's *t*-test. ACF, acriflavine.

VEGFR-1, HIF-2α, BNIP3, EDM1, and Serpine 1 after 24 hours of administration, with a further increase in potency observed at 20 μmol/L (►**Fig. 1B**). Concurrently, the reference compound PT2385 also repressed the expression of these genes in the same experiment, thereby validating the assay conditions. Angiogenesis is primarily mediated by VEGF signaling, initiated when VEGF ligands bind to their cognate membrane-bound receptors (VEGFR) on the surface of endothelial cells.[23] HST3782 downregulated HIF-targeted genes, suggesting its potential to inhibit angiogenesis.[24,25]

Next, we explored a synthetic route of HST3782 as illustrated in **Scheme 1**. The phenyl-1,3,4-triazole core (**5**) was generated in a diazonium reaction starting with 2,6-dichloroaniline (**1**) and methyl-2-chloro-2-(2-(2,6-dichlorophenyl)hydrazineylidene) acetate (**2**), followed by cyclization in the presence of freshly prepared isobutyraldehyde oxime (**4**). The methyl ester group in **5** was hydrolyzed by sodium hydroxide solution to yield the carboxylic acid **6**. It was then condensed with 8-azabicyclo [3.2.1]octan-3-one, leading to the amide compound **7**, the ketone group of which was reduced to give the final products, HST3782 and **8b**, as a pair of endo–exo isomers, which can be easily separated by chromatography (►**Fig. 2**). The conformations of isomers were confirmed through two-dimensional nuclear overhauser effect (2-D NOE) analysis of 2D 1H-1H nuclear overhauser effect spectroscopy (NOESY). It was observed that the H_{26} hydrogen atom of HST3782 with a chemical shift of around 3.93 ppm, is coupled to the four hydrogens on C_{22} and C_{23} (chemical shifts of around 1.73 (2H) and 1.97 (2H)) and did not show a NOE correlation with hydrogens on C_{18} and C_{19}. This indicates that the configuration of HST3782 is endo. In contrast, the 2D-NOESY of exo isomer, **8b**, displayed NOE correlations between H_{25} (chemical shift = 3.98) and hydrogens on C_{18} and C_{19} (chemical shift = 1.5). In addition, the ^{1}H NMR (nuclear magnetic resonance spectra) of HST3782 and **8b** exhibited differences in the chemical shift and coupling constant of hydrogen on the bridged ring (►**Fig. 2C**).

Next, the *in vivo* efficacy of HST3782 against angiogenesis was evaluated in the well-established zebrafish model. AB-strain zebrafish were bred and fertilized eggs were collected. Healthy zebrafish embryos at 6-hour postfertilization (hpf) were carefully selected under a dissecting microscope and distributed into 24-well plates, with 10 embryos per well. In multidosed toxicity evaluation, both HST3782 and compound **8b** showed no obvious toxicity (►**Fig. 3A**), and the mortality rates after 96 hours of drug exposure were less than 10%, even at a maximum concentration of 500 μmol/L. The malformation rates were assessed from 24 to 96 hours, and concentration-dependent and time-cumulative effects were illustrated (►**Fig. 3B**). Subsequent angiogenesis experiments were conducted at concentrations of 31.25, 62.5, and 125 μmol/L, with the highest experimental concentration representing 1/10 to 1/3 of the EC_{50} value that does not cause malformation. Subsequently, the intersegmental vessels (ISV) number was counted for the blank control group and drug-treated groups at 48 hpf, corresponding to the 24-hour drug administration period. At this stage, only the ISV can be counted, while the subintestinal vessels (SIV) have not yet developed. As illustrated in ►**Fig. 3C**, HST3782 inhibited the dorsal ISV development by 12 and 14%, respectively, at 62.5 and 125 μmol/L; whereas **8b** showed no significant effect. At 48 hours, the areas of SIV were analyzed. As shown in ►**Fig. 3D**, HST3782 significantly and dosed-dependently inhibited abdominal SIV development, with inhibition rates being 26, 45, and 56%, respectively, at 31.25, 62.5, and 125 μmol/L, whereas its exo isomer **8b**

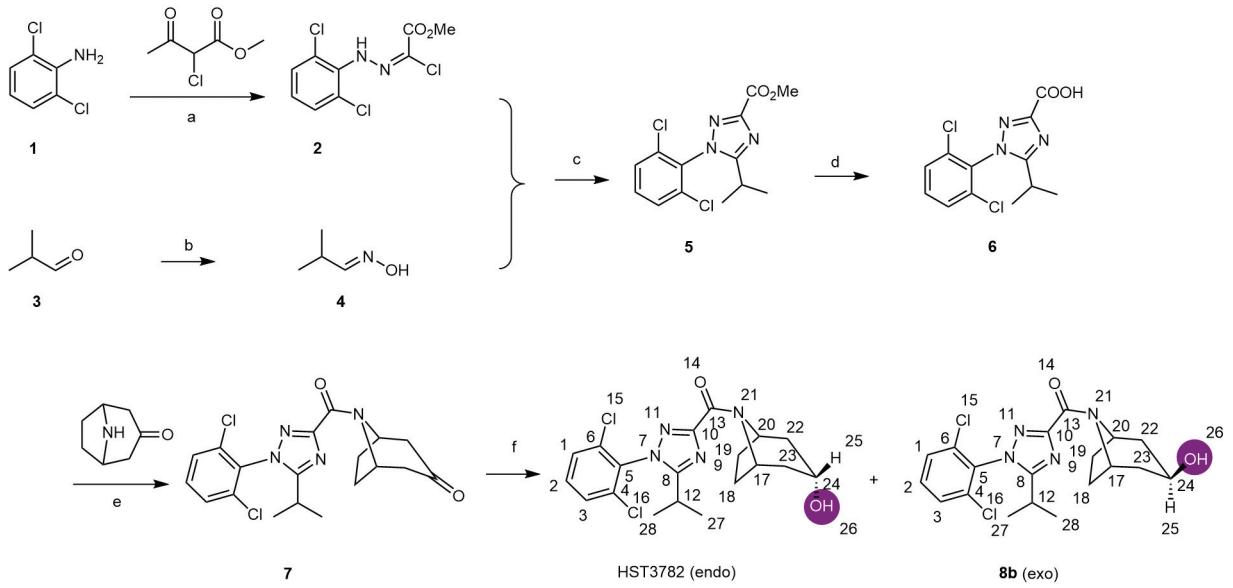

Scheme 1 The synthetic route of HST3782 and its isomer. Reagents and conditions: (**a**) $NaNO_2$, HCl, MeOH, r.t., 12 hours; (**b**) $NH_2OH \cdot HCl$, toluene, r.t., 30 minutes; (**c**) TEA, toluene, 120°C, 2 hours, 42.1%; (**d**) 2 mol/L NaOH, MeOH/H_2O, r.t., 2 hours, 92.0%; (**e**) TBTU, DIPEA, DCM, r.t., 12 hours, 50.1%; (**f**) $NaBH_4$, MeOH, r.t., 2 hours, 17.1%.

exhibited reduced inhibitory effects. Both the results of zebrafish ISV and SIV development demonstrated that HST3782 exhibited inhibitory effects on zebrafish vasculature and the exo isomer **8b** has reduced activity.

Conclusion

The HIF pathway serves as the master regulator of angiogenesis and other tissue-specific functions by sensing O_2 homeostasis. It plays a crucial role in the formation of new blood vessels in both physiological and pathophysiological settings. Targeting the HIF–VEGF axis has emerged as a promising approach for angiogenesis-related diseases, including cancer.[26] In this study, we identified HST3782 as an HIF signal inhibitor with a bridged bicyclic scaffold through dual reporter assays in 786-O cells and SUM159 cells. It reduced the expression of HIF downstream genes including VEGFa and VEGFR, which are key drivers of angiogenesis. Studies in the zebrafish model further confirmed the inhibitory effect of HST3782 on angiogenesis. Furthermore, the endoconfiguration of the compound is superior for bioactivity relative to its exo isomer **8b**. We identified HST3782 as an interesting HIF signal inhibitor with a novel 3-hydroxy-8-azabicyclo[3.2.1]octane bridge scaffold, and further studies are necessary to use HST3782 as a lead compound to exploring novel agents for antiangiogenetic therapy.

Experimental Section

General Conditions

All reagents and solvents were used directly as purchased from commercial sources. Flash chromatography was performed using silica gel (200–300 mesh). All reactions were monitored by thin-layer chromatography, using silica gel plates with fluorescence F_{254} and UV light visualization. ^1H NMR and ^{13}C NMR spectra were recorded on a Bruker AV-400 spectrometer (Bruker, Billerica, United States). Coupling constants (J) are expressed in hertz (Hz). Chemical shifts (δ) of NMR are reported in parts per million (ppm) units relative to an internal control (trimethylsilane). Electrospray ionization mass spectrometry were recorded on an Agilent 1200 HPLC-MSD mass spectrometer (Agilent, Santa Clara, United States).

Synthesis of Methyl 1-(2,6-dichlorophenyl)-5-isopropyl-1*H*-1,2,4-triazole-3-carboxylate (Compound 5)

2,6-dichloroaniline (1.4 g, 9 mmol, 1 equiv.) was dissolved in MeOH (8 mL). Sodium nitrite aqueous solution (1.2 g, 18 mmol, 2 equiv.) was added slowly. The resulting mixture was stirred for 15 minutes and adjust the pH to 3-4 with sodium acetate. Methyl 2-chloro-3-oxobutanoate (1.1 mL, 9 mmol, 1 equiv.) was added. The mixture was continuously stirred for 12 hours at room temperature, quenched with water, and then extracted with ethyl acetate three times. The combined organic layers were washed with saturated NaCl solution and concentrated to give compound **2** as a yellow solid, which was used directly without further purification.

To a solution of isobutyraldehyde (0.6 g, 9 mmol, 1 equiv.) in toluene (30 mL) was added hydroxylamine hydrochloride (0.6 g, 9.9 mmol, 1 equiv.). The mixture was stirred at room temperature for 30 minutes. Compounds **2** and Et_3N (2.5 mL) were added. The reaction was refluxed at 120°C for 2 hours. After completion of the reaction, toluene was removed by vacuum rotary evaporation. The residue was washed with saturated NaCl solution, extracted with EtOAc, and purified by column chromatography (ethyl acetate: petroleum ether = 1:5) to give compound **5** (120 mg, 42.1%) as a yellow solid.

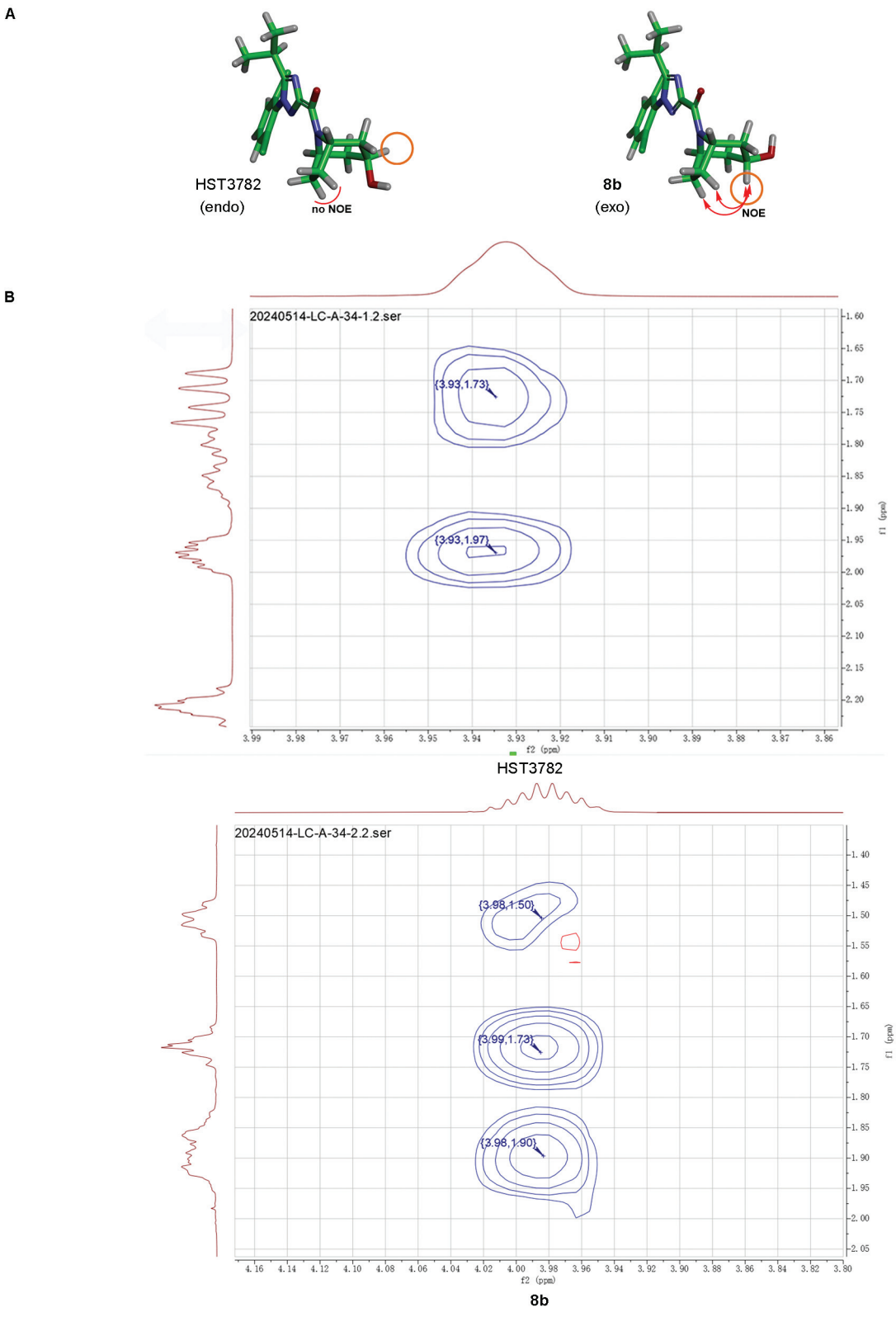

Fig. 2 (**A**) Structure, (**B**) 2D-NOESY spectra, and (**C**) ^{1}H NMR spectra of HST3782 and **8b**.

Synthesis of 1-(2,6-dichlorophenyl)-5-isopropyl-1*H*-1,2,4-triazole-3-carboxylic Acid (Compound 6)

Compound **5** (500 mg, 1.5 mmol) was dissolved in MeOH, and sodium hydroxide aqueous solution (2 mol/L, 20 mL) was added. The mixture was stirred at room temperature for 2 hours. After completion of the reaction, the pH was adjusted to 3 to 4 with hydrochloric acid until a solid precipitate appeared, which was isolated by suction filtration, giving compound **6** (437 mg, 92.0%) as a white solid.

continued

C

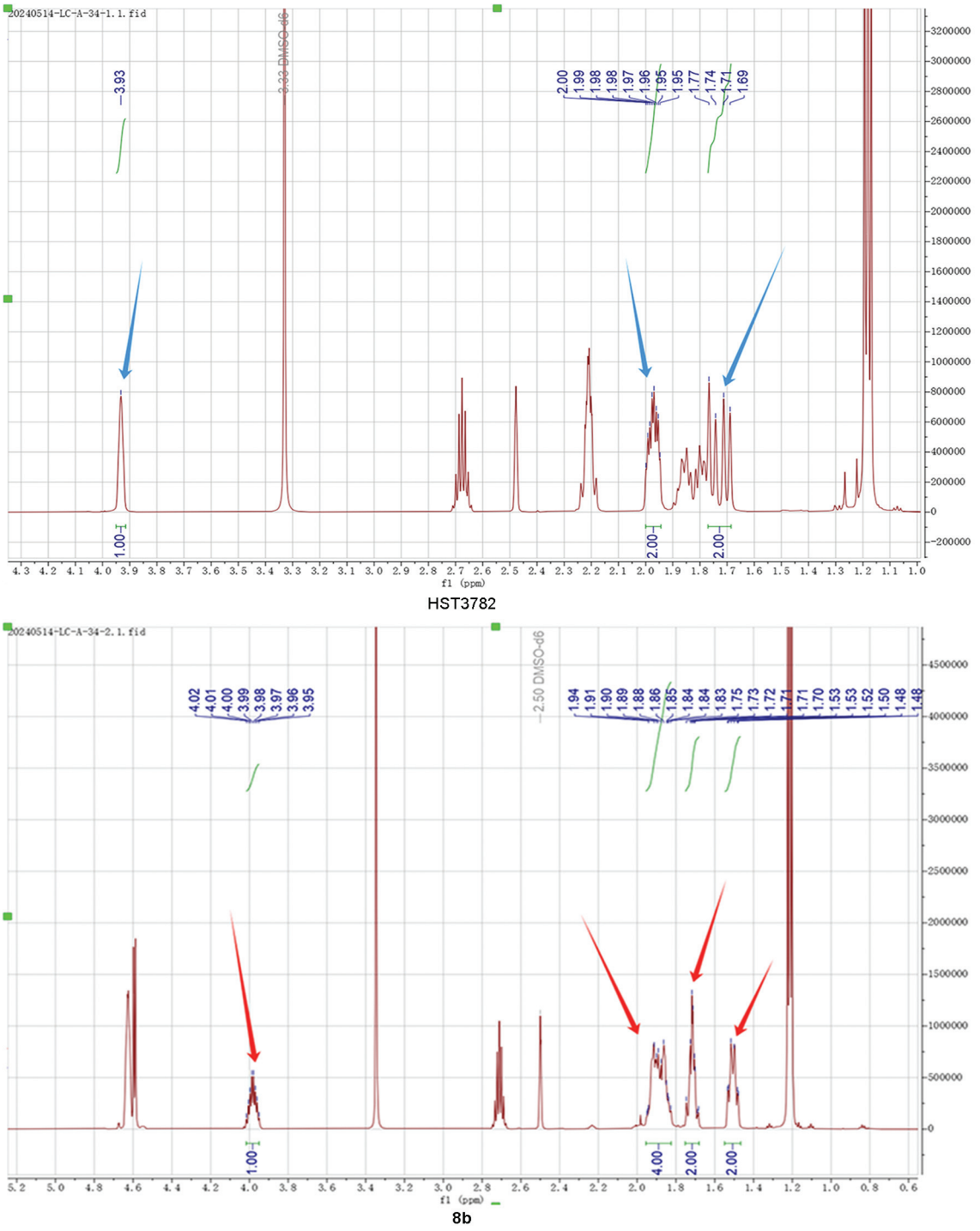

Fig. 2 (*Continued*)

Synthesis of 8-(1-(2,6-dichlorophenyl)-5-isopropyl-1*H*-1,2,4-triazole-3-carbonyl)-8-azabicyclo[3.2.1]octan-3-one (Compound 7)

Compound **6** (400 mg, 1.3 mmol, 1 equiv.) was dissolved in dichloromethane at 0°C, followed by the addition of TBTU (429 mg, 1.3 mmol, 1 equiv.) and DIPEA (N, N-Diisopropylethylamine; 1.4 mL, 6 equiv.). The mixture was stirred at room temperature for 12 hours, washed with an ammonium chloride aqueous solution upon completion of the reaction, and extracted with dichloromethane. The organic layers were concentrated. The residue was purified by column chromatography (ethyl acetate:petroleum ether = 1:2) to give compound **7** (271 mg, 50.1%) as a white solid.

Synthesis of HST3782 and 8b

Compound **7** (200 mg, 0.5 mmol, 1 equiv.) was dissolved in MeOH. Sodium borohydride was added slowly. The reaction was stirred at room temperature for 2 hours and quenched

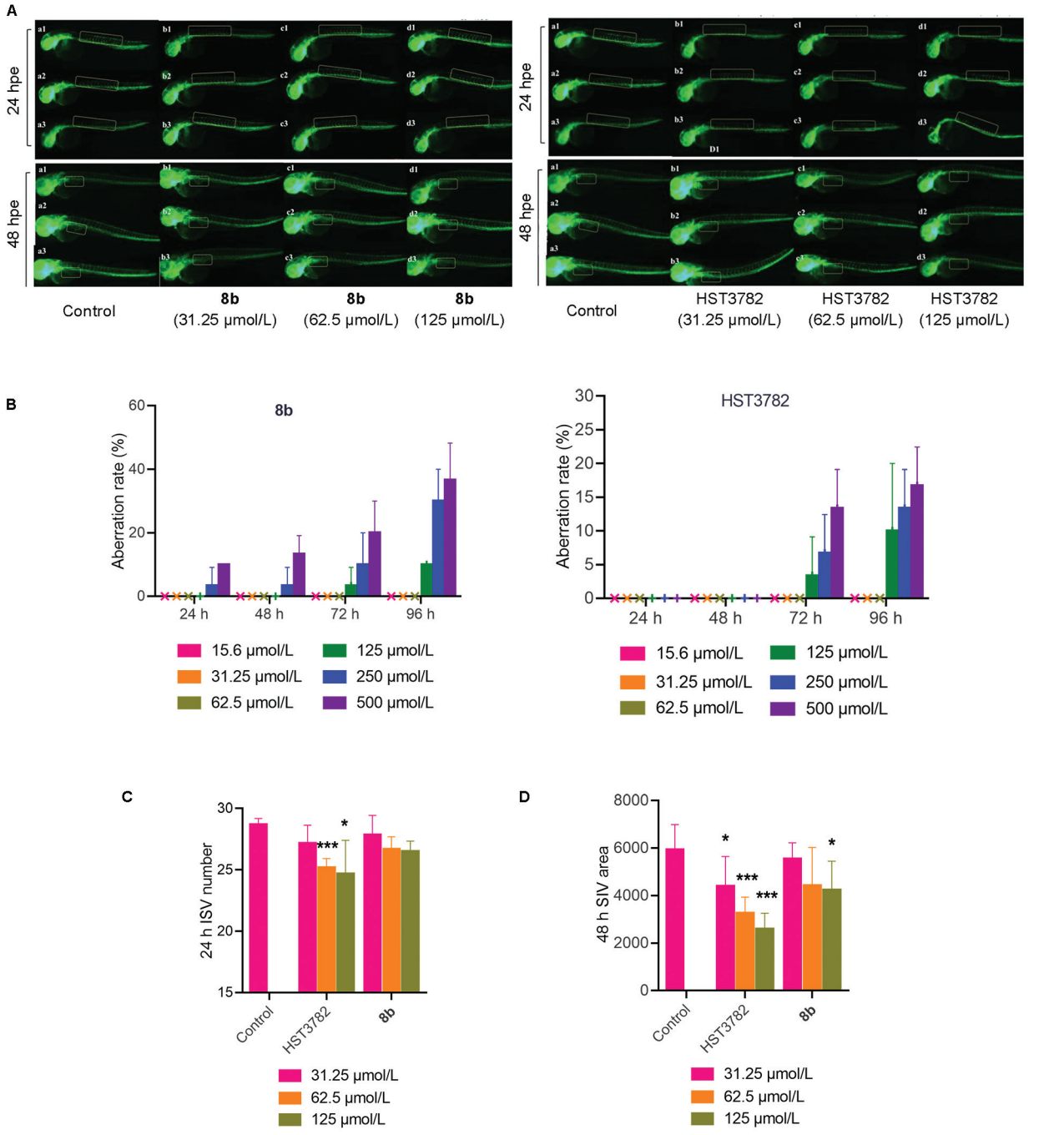

Fig. 3 Anti-angiogenetic efficacy of HST3782 in zebrafish models. (**A**) The representative image of vascular suppression in the control group, **8b** or HST3782 at the concentration of 31.25, 62.5, and 125 μmol/L, at the indicated time, respectively (magnification: 4 ×). The yellow dashed box represents the position of ISV and SIV. The malformation rate (**B**), ISV number (**C**), and SIV area (**D**) were analyzed at the indicated time. Data are expressed as the mean ± standard deviation ($n = 10$). $^{*}p < 0.05$, $^{**}p < 0.01$, $^{***}p < 0.001$ versus the DMSO control group, analyzed by two-tailed Student's *t*-test. ISV, intersegmental vessels; SIV, subintestinal vessels.

with ammonium chloride. The mixture was extracted with EtOAc. The organic layers were concentrated. The residue was purified by column chromatography (ethyl acetate: petroleum ether = 1:2) to give HST3782 and **8b**, as a pair of endo–exo isomers.

HST3782, chemically named "endo-(1-(2,6-dichlorophenyl)-5-isopropyl-1*H*-1,2,4-triazol-3-yl)(3-hydroxy-8-azabicyclo[3.2.1]octan-8-yl)methanone." ^{1}H NMR (600 MHz, dimethylsulfoxide [DMSO]-d_6) δ 7.83 (d, $J = 8.2$ Hz, 2H), 7.76–7.70 (m, 1H), 4.68 (d, $J = 2.5$ Hz, 1H), 4.61 (dt, $J = 6.8$, 3.0 Hz, 1H), 4.56 (dt, $J = 6.7$, 3.0 Hz, 1H), 3.98–3.95 (m, 1H), 2.71 (p, $J = 6.8$ Hz, 1H), 2.28–2.20 (m, 2H), 2.00 (ddt, $J = 13.7$, 8.7, 4.3 Hz, 2H), 1.91–1.79 (m, 2H), 1.78–1.70 (m, 2H), 1.21 (dd, $J = 8.0$, 6.8 Hz, 6H). ^{13}C NMR (151 MHz, DMSO) δ 162.98, 158.19, 156.63, 133.90 (2C), 132.11, 130.07 (2C), 63.34, 55.43, 51.63, 40.70, 38.80, 28.77, 26.99, 26.20, 21.39, 21.34 (2C). MS-ESI (*m*/*z*) calcd. for $C_{19}H_{23}Cl_2N_4O_2$ $[M+H]^+$ 409.1120, found: 409.1237.

8b, chemically named "exo-(1-(2,6-dichlorophenyl)-5-isopropyl-1*H*-1,2,4-triazol-3-yl)(3-hydroxy-8-azabicyclo [3.2.1]octan-8-yl)methanone." ^{1}H NMR (600 MHz, DMSO-d_6) δ 7.84 (d, J = 8.2 Hz, 2H), 7.73 (dd, J = 8.7, 7.7 Hz, 1H), 4.63 (h, J = 3.0 Hz, 2H), 4.60 (d, J = 6.1 Hz, 1H), 3.99 (tq, J = 11.4, 6.0 Hz, 1H), 2.72 (hept, J = 6.8 Hz, 1H), 1.97-1.81 (m, 4H), 1.73 (qd, J = 8.7, 7.5, 2.8 Hz, 2H), 1.56-1.47 (m, 2H), 1.22 (t, J = 6.8 Hz, 6H). ^{13}C NMR (151 MHz, DMSO) δ 163.04, 158.14, 156.88, 133.88, 133.83 (2C), 132.09, 130.08 (2C), 62.24, 55.40, 51.93, 42.75, 40.88, 28.75, 27.00, 26.21, 21.40, 21.36 (2C). MS-ESI (m/z) calcd. for $C_{19}H_{23}Cl_2N_4O_2$ $[M+H]^+$ 409.1120, found: 409.1197.

Hypoxia Response Element Dual Luciferase Reporter Assay in 786-O cells

786-O cells (ATCC, Madison, United States) were seeded in 96-well plates at a density of 7,000 cells/well and transfected when they reached 80 to 85% confluency. The transfections use 0.5 μg HRE-Luc2 vector (Promega, #E4001, Madison, United States) mixed with 0.05 μg Renilla-pGL DNA (Promega, #E1741, Madison, United States) and 0.825 μL lipofectamine 2000 transfection reagent (Thermo Fisher Scientific, #11668030, Agawam, United States) in a 10 μL Opti-MEM medium per well. The mixtures were cultured for 20 minutes. The complexes (10 μL) were directly added to cells in a reduced serum medium. Approximately 6 hours of posttransfection, PT2385 (TargetMol Chemicals, #T7848, Shanghai, China) or HST3782 was added. At 24 hours of posttransfection, a dual luciferase reporter assay kit (Promega #E1960, Madison, United States) was used to determine the luciferase activity of the cells according to the manufacturer's introduction to assess the activation of HIF signaling.

Hypoxia Response Element Dual Luciferase Reporter Assay in SUM159 cells

SUM159 cells (kindly provided by Prof. Haiquan Lv from Shandong University) were stably transfected with reporter plasmid pHRE-SV-Firefly and control plasmid pSV-Renilla using PolyJet (SignaGen, Rockville, United States). 1×10^4 transfected SUM159 cells were seeded in each well of 96-well plate and cultured under 21% or 1% O_2 in the presence of indicated doses of HST3782, acriflavine (TargetMol Chemicals, T19832, Shanghai, China), or DMSO (as control) for 3 days. The ratio of Firefly/Renilla luciferase activity was determined by using the dual luciferase reporter assay kit on Centro LB960 microplate luminometer (Berthold, Ringtunveien, Norway).

RNA Isolation and Quantitative Real-Time Polymerase Chain Reaction

786-O cells (ATCC, Madison, United States) were seeded in 12-well plates, treated with PT2385 (10 μmol/L), HST3782 (0 μmol/L), or HST3782 (20 μmol/L) in a reduced serum medium for 24 hours, and then washed with phosphate buffer saline. Total RNA was isolated by Trizol (Beyotime, #R0016, Shanghai, China). RT-PCRs were performed in triplicate using standard SYBR green reagents. The primer sequences used for quantitative PCR are as follows: erythropoietin (EPO)_fwd, AACAATCACTGCTGACACTT; EPO_rev, AGAGTTGCTCTCTGGACAGT; VEGFa_fwd, AGGGCAGAATCATCACGAAGT; VEGFa_rev, AGGGTCTCGATTGGATGGCA; Serpine1_fwd, ACCGCAACGTGGTTTTCTCA; Serpine1_rev, TTGAATCCCATAGCTGCTTGAAT; HIF-2α_fwd, CGGAGGTGTTCTATGAGCTGG; HIF-2α_rev, AGCTTGTGTGTTCGCAGGAA. VEGFR-1_fwd, TTTGCCTGAAATGGTGAGTAAGG; VEGFR-1_rev, TGGTTTGCTTGAGCTGTGTTC; BNIP3_fwd, CAGGGCTCCTGGGTAGAACT; BNIP3_rev, CTACTCCGTCCAGACTCATGC; EDM1_fwd, GATCACGTTCCTGAAAAACACG; EDM1_rev, GCTCTCCGTCTGGATGCAG.

Antiangiogenesis in Zebrafish

Transgenic zebrafish embryos with the background of the AB strain expressing Tg (Fli: EGFP) were used in the experiment according to a reported study.[27] Healthy zebrafish embryos at 6 hpf were selected under a dissecting microscope and placed in 24-well plates at a density of 10 embryos per well. For embryo toxicity testing, the experimental groups included a DMSO control group and six working concentrations (15.6, 31.25, 62.5, 125, 250, and 500 μmol/L) for each compound. Drug administration started at 24 hpf. Mortality and deformity rates of embryos were recorded at 24, 48, 72, and 96 hours, respectively. For vasculature development evaluation, the experimental groups included a solvent control group (3.2% DMSO) and three working concentrations (31.25, 62.5, and 125 μmol/L) for each compound, with three replicates for each concentration gradient. After 24 and 48 hours of exposure, zebrafish were captured with a fluorescence microscopy system (Nikon Ci-S), and the number of ISV and area of SIV were measured.

Data Analysis

The results are represented as means with respective standard errors. Data analysis was performed with GraphPad Prism Software (GraphPad Software Inc., version 8). Student's t-test or one-way analysis of variance with Brown–Forsythe was utilized for statistical analysis. Significant differences were indicated by asterisks considering p-values < 0.05.

Funding
This work was supported by the National Natural Science Foundation of China (Grant No. 82204194) and the Guangdong Education Department (Grant No. 2022KTSCX107).

Conflict of Interest
None declared.

References

1 Semenza GL. Hypoxia-inducible factors in physiology and medicine. Cell 2012;148(03):399–408
2 Goldberg MA, Schneider TJ. Similarities between the oxygen-sensing mechanisms regulating the expression of vascular endothelial growth factor and erythropoietin. J Biol Chem 1994;269 (06):4355–4359

3 Wu D, Potluri N, Lu J, Kim Y, Rastinejad F. Structural integration in hypoxia-inducible factors. Nature 2015;524(7565):303–308
4 Wang GL, Jiang BH, Rue EA, Semenza GL. Hypoxia-inducible factor 1 is a basic-helix-loop-helix-PAS heterodimer regulated by cellular O_2 tension. Proc Natl Acad Sci U S A 1995;92(12): 5510–5514
5 Ema M, Taya S, Yokotani N, Sogawa K, Matsuda Y, Fujii-Kuriyama Y. A novel bHLH-PAS factor with close sequence similarity to hypoxia-inducible factor 1alpha regulates the VEGF expression and is potentially involved in lung and vascular development. Proc Natl Acad Sci U S A 1997;94(09):4273–4278
6 Markolovic S, Wilkins SE, Schofield CJ. Protein hydroxylation catalyzed by 2-oxoglutarate-dependent oxygenases. J Biol Chem 2015;290(34):20712–20722
7 Salceda S, Caro J. Hypoxia-inducible factor 1α (HIF-1α) protein is rapidly degraded by the ubiquitin-proteasome system under normoxic conditions. Its stabilization by hypoxia depends on redox-induced changes. J Biol Chem 1997;272(36):22642–22647
8 Hogenesch JB, Chan WK, Jackiw VH, et al. Characterization of a subset of the basic-helix-loop-helix-PAS superfamily that interacts with components of the dioxin signaling pathway. J Biol Chem 1997;272(13):8581–8593
9 Downes NL, Laham-Karam N, Kaikkonen MU, Ylä-Herttuala S. Differential but complementary HIF1α and HIF2α transcriptional regulation. Mol Ther 2018;26(07):1735–1745
10 Genbacev O, Zhou Y, Ludlow JW, Fisher SJ. Regulation of human placental development by oxygen tension. Science 1997;277 (5332):1669–1672
11 Cho H, Du X, Rizzi JP, et al. On-target efficacy of a HIF-2α antagonist in preclinical kidney cancer models. Nature 2016; 539(7627):107–111
12 Deeks ED. Belzutifan: First Approval. Drugs 2021;81(16): 1921–1927
13 Beppu K, Nakamura K, Linehan WM, Rapisarda A, Thiele CJ. Topotecan blocks hypoxia-inducible factor-1alpha and vascular endothelial growth factor expression induced by insulin-like growth factor-I in neuroblastoma cells. Cancer Res 2005;65(11):4775–4781
14 Falchook GS, Wheler JJ, Naing A, et al. Targeting hypoxia-inducible factor-1α (HIF-1α) in combination with antiangiogenic therapy: a phase I trial of bortezomib plus bevacizumab. Oncotarget 2014;5 (21):10280–10292
15 Befani CD, Vlachostergios PJ, Hatzidaki E, et al. Bortezomib represses HIF-1α protein expression and nuclear accumulation by inhibiting both PI3K/Akt/TOR and MAPK pathways in prostate cancer cells. J Mol Med (Berl) 2012;90(01):45–54
16 Abd-Aziz N, Stanbridge EJ, Shafee N. Bortezomib attenuates HIF-1- but not HIF-2-mediated transcriptional activation. Oncol Lett 2015;10(04):2192–2196
17 Mangraviti A, Raghavan T, Volpin F, et al. HIF-1α- targeting acriflavine provides long term survival and radiological tumor response in brain cancer therapy. Sci Rep 2017;7(01):14978
18 Naik R, Won M, Kim BK, et al. Synthesis and structure-activity relationship of (*E*)-phenoxyacrylic amide derivatives as hypoxia-inducible factor (HIF) 1α inhibitors. J Med Chem 2012;55(23): 10564–10571
19 Xu H, Wang J, Chen Y, et al. Design, synthesis and evaluation of the novel chalcone derivatives with 2,2-dimethylbenzopyran as HIF-1 inhibitors that possess anti-angiogenic potential. Eur J Med Chem 2023;250:115171
20 Xu XL, Yang YR, Mo XF, Wei JL, Zhang XJ, You QD. Design, synthesis, and evaluation of benzofuran derivatives as novel anti-pancreatic carcinoma agents via interfering the hypoxia environment by targeting HIF-1α pathway. Eur J Med Chem 2017;137:45–62
21 Wehn PM, Rizzi JP, Dixon DD, et al. Design and activity of specific hypoxia-inducible factor-2α (hif-2α) inhibitors for the treatment of clear cell renal cell carcinoma: discovery of clinical candidate (*S*)-3-((2,2-difluoro-1-hydroxy-7-(methylsulfonyl)-2,3-dihydro-1*H*-inden-4-yl)oxy)-5-fluorobenzonitrile (PT2385). J Med Chem 2018;61(21):9691–9721
22 Liu Q, Guan C, Liu C, Li H, Wu J, Sun C. Targeting hypoxia-inducible factor-1alpha: A new strategy for triple-negative breast cancer therapy. Biomed Pharmacother 2022;156:113861
23 Li Y, Pasunooti KK, Peng H, et al. Design and synthesis of tetrazole- and pyridine-containing itraconazole analogs as potent angiogenesis inhibitors. ACS Med Chem Lett 2020;11(06):1111–1117
24 Carmeliet P. Angiogenesis in life, disease and medicine. Nature 2005;438(7070):932–936
25 Carmeliet P, Dor Y, Herbert JM, et al. Role of HIF-1α in hypoxia-mediated apoptosis, cell proliferation and tumour angiogenesis. Nature 1998;394(6692):485–490
26 Choueiri TK, Kaelin WG Jr. Targeting the HIF2-VEGF axis in renal cell carcinoma. Nat Med 2020;26(10):1519–1530
27 Cheng H, Zhang L, Liu Y, et al. Design, synthesis and discovery of 5-hydroxyaurone derivatives as growth inhibitors against HUVEC and some cancer cell lines. Eur J Med Chem 2010;45(12): 5950–5957